

Obtaining shear wave input for 1d site response analysis: a frequency adjustment method based on strong motion records – part i: formulation and theoretical validation

Yiping Wang¹, Yinfeng Dong², Yilin Wang³, Yiming Xie⁴, Fuchao Cao⁵

Key Laboratory of New Technology for Construction of Cities in Mountain Area, Chongqing University, Chongqing, China

School of Civil Engineering, Chongqing University, Chongqing, China

¹Corresponding author

E-mail: ¹1580403229@qq.com, ²dongyinfeng@cqu.edu.cn, ³2656405341@qq.com, ⁴754522870@qq.com, ⁵caofuchaovvv@163.com

Received 13 August 2025; accepted 10 November 2025; published online 22 December 2025
DOI <https://doi.org/10.21595/vp.2025.25272>



74th International Conference on Vibroengineering in Tashkent, Uzbekistan, November 27-29, 2025

Copyright © 2025 Yiping Wang, et al. This is an open access article distributed under the Creative Commons Attribution License, which permits unrestricted use, distribution, and reproduction in any medium, provided the original work is properly cited.

Abstract. Significant discrepancies exist between strong motion records and the actual incident wave field across frequency bands, impacting wave propagation analysis accuracy. This paper proposes a frequency-domain adjustment method (AWIM) to derive realistic incident wave fields from recorded motions. The method constructs site-specific frequency adjustment curves by analyzing the steady-state response of soil layers to harmonic excitations using wave propagation theory and recursive calculations of reflection/transmission across layers. Results reveal that soft soil sites exhibit strong frequency-dependent effects: low-frequency waves undergo significant amplification (nearly twice the incident wave amplitude), while high-frequency waves show complex interactions – distinct bands experience notable amplification or attenuation.

Keywords: wave propagation, seismic wavefield, site response, strong motion records, incident wave.

1. Introduction

For one-dimensional seismic response analysis, the main approaches include the Vibration Input Method (VIM) based on structural dynamics theory [1], the Wave Input Method (WIM) grounded in wave propagation theory [2], and the Finite Element Method (FEM) that uses numerical discretization to solve wave motion equations [3]. Among these, the wave input method (WIM) is particularly effective for analyzing multi-layered soil media and complex seismic wave fields [4]. It treats seismic waves as disturbances propagating through soil layers and calculates their propagation and response using transfer matrices [5] or wave equations. However, a key challenge arises when using borehole or bedrock acceleration records as input for WIM. These records represent a total wave field, including both incident and reflected waves, rather than the idealized incident wave field required for accurate wave propagation analysis. This discrepancy, especially prominent in low-frequency displacement responses, significantly limits the accuracy of site response analysis using conventional WIM. To address this issue, we propose a frequency-domain adjustment method (AWIM) to derive realistic incident wave fields from recorded motions.

2. Incident wave adjustment method

2.1. One-dimensional wave propagation analysis

The assumptions based on this paper are: one-dimensional layered medium, SH wave, linear

elasticity, top free surface, and semi infinite substrate. Some parameters of soil involved are shown in Table 1.

Fig. 1 illustrates the wave propagation path in a one-dimensional soil system. In this study, each soil layer is treated as a homogeneous medium, with its density, shear wave velocity, thickness, and single wave propagation time in the soil layer denoted as ρ_i , $v_{s,i}$, h_i , and τ_i ($i = 1, 2, \dots, n$), respectively. As shown in Fig. 1(c), when a shear wave propagates from the i th layer to the $(i + 1)$ th layer, its reflection coefficient is denoted as $\beta_{1,i}$; when propagating from the i th layer to the $(i - 1)$ th layer, the reflection coefficient is denoted as $\beta_{2,i}$. The relation between above coefficients is given by:

$$-\beta_{2,i+1} = \beta_{1,i} = \frac{\rho_i v_{s,i} - \rho_{i+1} v_{s,i+1}}{\rho_i v_{s,i} + \rho_{i+1} v_{s,i+1}}, \quad i = 1, 2, \dots, n - 1. \quad (1)$$

For the ground surface (the n th layer), it is assumed to be a perfect reflector. And for the bottommost layer of soil (the 1st layer), it is assumed to have no reflection.

Table 1. Soil parameters of numerical model

Density	Shear wave velocity	Thickness	Single wave propagation time in the soil layer	Reflection coefficient	Damping ratio	The first-order angular frequency
ρ	v_s	h	τ	β	ξ	ω

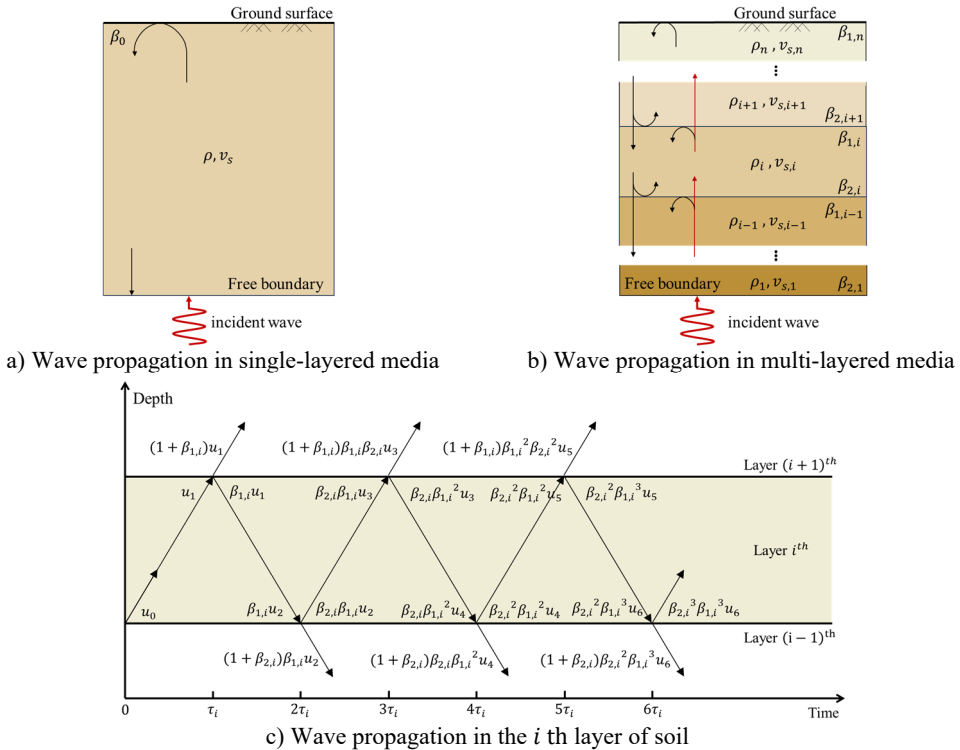


Fig. 1. Schematic diagram of the wave propagation model in soil

According to Fig. 1(c), the shear wave propagation from the bottom of the soil layer upward can be derived, including the wave responses at the top and bottom of each soil layer. The response at the top of the current layer and the transmitted shear wave into the upper layer can be expressed as:

$$p_{ru}^-(N\tau_i) = p_{tu}^-(N\tau_i) = (1 + \beta_{1,i}) \sum_{j=1}^N \exp(-(2j-1)\xi_i\omega\tau_i)(\beta_{1,i}\beta_{2,i})^{j-1}u_{2j-1}, \quad (2)$$

where, u_{2j-1} represents the shear wave in the soil layer that has shifted by $(2j-1)\tau_i$ phases relative to the incident wave u_0 ; N denotes the number of reflections of the shear wave in the soil layer, ξ_i and ω represent the damping ratio of the i th soil layer and the first-order angular frequency of the soil, respectively.

The reflected shear wave transmitted into the next soil layer p_{td}^- is:

$$p_{td}^-(N\tau_i) = (1 + \beta_{2,i})\beta_{1,i} \sum_{j=1}^N \exp(-2j\xi_i\omega\tau_i)(\beta_{1,i}\beta_{2,i})^{j-1}u_{2j}. \quad (3)$$

The response at the bottom of the current soil layer p_{rd}^- is:

$$p_{rd}^-(N\tau_i) = u_0 + p_{td}^-(N\tau_i). \quad (4)$$

Similarly, as the shear wave propagates downward from the top of the soil layer, the dynamic responses at both the top and bottom interfaces of each sublayer can be formulated as follows.

The response at the bottom of the current soil layer p_{tu}^+ and the transmitted shear wave into the next soil layer p_{td}^+ are expressed as:

$$p_{tu}^+(N\tau_i) = p_{td}^+(N\tau_i) = (1 + \beta_{2,i}) \sum_{j=1}^N \exp(-(2j-1)\xi_i\omega\tau_i)(\beta_{1,i}\beta_{2,i})^{j-1}u_{2j-1}. \quad (5)$$

The reflected shear wave transmitted into the previous soil layer p_{tu}^- is:

$$p_{tu}^-(N\tau_i) = (1 + \beta_{1,i})\beta_{2,i} \sum_{j=1}^N \exp(-2j\xi_i\omega\tau_i)(\beta_{1,i}\beta_{2,i})^{j-1}u_{2j}. \quad (6)$$

The response at the top of the current soil layer p_{ru}^+ is:

$$p_{ru}^+(N\tau_i) = u_0 + p_{tu}^-(N\tau_i). \quad (7)$$

To improve computational efficiency, this study sets the condition that wave propagation is terminated when the amplitude decays to less than 0.05 % of its original value due to damping. This threshold is expressed as $(\beta_{1,i}\beta_{2,i})^N \geq 0.05 \%$. Based on this threshold, the number of reflections N of the shear wave in the i th soil layer is $N \geq \frac{\lg 0.05\%}{\lg(\beta_{1,i}\beta_{2,i})} \approx \frac{-3.3}{\lg(\beta_{1,i}\beta_{2,i})}$. By using above equations, the propagation of shear waves in the soil and the responses of each soil layer can be calculated using a recursive method.

2.2. Model validation

To assess the accuracy of the proposed model, a 500-meter soil column was extracted from a semi-infinite space and discretized into 1-meter elements. The soil properties were defined as a density of 2200 kg/m³ and a shear wave velocity of 200 m/s. A unit pulse shear displacement wave was introduced vertically upward at the base of the column, as shown in Fig. 2(a). Based on one-dimensional wave propagation theory, the shear wave reaches the midpoint of the column at 1.25 seconds ($250/200 = 1.25$), arrives at the top at 2.5 seconds ($500/200 = 2.5$), and is amplified by a factor of two due to the free surface at the top. The wave then reflects off the top surface and propagates downward, reaching the midpoint again at 3.75 seconds ($750/200 = 3.75$) and the base at 5 seconds ($1000/200 = 5$). After 7.0 seconds ($1000/200+2 = 7.0$), the shear wave completely

exits the base and propagates to infinity. Following this, the displacement of each part of the model is calculated to be zero. The horizontal displacement response solutions at the bottom, middle, and top of the model are illustrated in Figs. 2(b) and 2(c) for damping coefficients of 0 and 400 kg/m³/s, respectively.

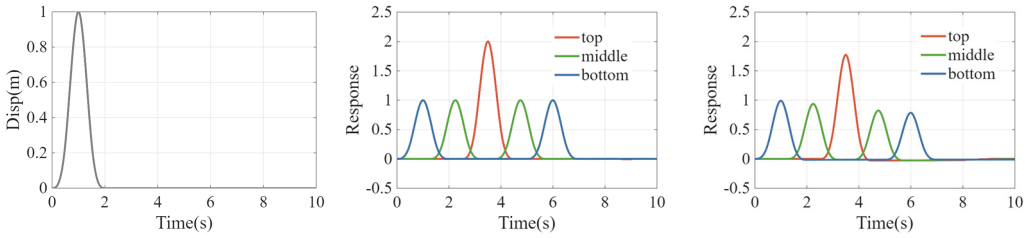


Fig. 2. Model validation case

2.3. Incident wave adjustment method

For single-layer or multi-layer soils, when the frequency of the incident wave satisfies a specific multiple (or ratio) relationship with the natural frequency of the soil, the phase difference between the reflected and incident waves can cause amplification or attenuation of the wave field amplitude. Therefore, by analyzing the response of the site to harmonic excitations of different frequency, a specific frequency adjustment coefficient for the site can be obtained.

To determine the frequency adjustment coefficient of the soil, assume the soil layer thickness is h , the shear wave velocity is v_s , the density is ρ , and the damping ratio is ξ . A set of sine waves with different frequencies (amplitude set to 1) is input at the bottom of the soil layer. Based on wave theory and using the method described in above Section 2.1, the response at the bottom of the soil layer to the harmonic excitations of different frequency is calculated. The specific steps are as follows

(1) Determine the reflection and transmission coefficients β . The reflection coefficient at the top of the soil is defined $\beta = 1$, indicating total reflection.

(2) Time delay and propagation process. The time delay τ for the seismic wave propagation through the soil layer is determined by the layer thickness h and the shear wave velocity v_s , i.e., $\tau = h/v_s$. The time delay determines the duration for both the reflected and transmitted waves to propagate through the soil layer, which in turn affects the frequency response characteristics.

(3) Input sine waves with different frequency. To study the response of a single-layer soil, a set of sine waves with different frequencies is chosen as the input wave. The expression for the input wave is given by:

$$x_{in}(t) = \sin(2\pi f_i t), \quad t \in [0, T], \quad (8)$$

where f_i is the frequency of the input wave, and T is the total duration of the wave. After analyzing a large number of examples, it is recommended that the total duration T should be at least ten sine wave periods to ensure the calculation accuracy. And to prevent the propagation time of high-frequency sine waves from being too short, we will increase the total duration by two seconds. In summary, T should satisfy as $T \geq \frac{(2+10t_p f_i)}{f_i}$, where 2 represents two seconds of increase, and $10t_p f_i$ represents ten sine wave periods. The number of time steps n should meet the requirement that each sine wave is divided into a or more parts:

$$n \geq \frac{a(2 + 10t_p f_i)}{f_i \tau_{min}}, \quad (9)$$

where t_p is one-quarter of the inherent period of the soil, which can be simplified as $t_p = \sum_{i=1}^n \frac{h_i}{v_{s,i}}$, τ_{min} is the minimum propagation time of soil wave for each layer, and a is the number of time steps in one cycle of the sine wave. In the equation, n is dimensionless, and the algorithm is more stable when $a \geq 20$.

(4) Frequency adjustment coefficient. After the input wave propagates through the soil layers, it undergoes multiple reflections and transmissions, and its energy gradually reaches a steady state. By numerical simulation, the wave response at the bottom of the soil is calculated for different frequency sine wave inputs, and the steady-state amplitude of the signal is extracted, defined as the frequency domain amplification coefficient $\zeta(f)$:

$$\zeta(f) = \frac{|x_{re}|}{|x_{in}|}, \quad (10)$$

where $|x_{in}|$ represents the amplitude of the input sine wave, and $|x_{re}|$ denotes the amplitude of the envelope of the steady-state signal which includes the incident wave. To obtain the steady-state response, the envelope of the signal is extracted using the Hilbert transform (HT). The result of the Hilbert transform is given by $Env(t) = |x(t) + i * H(x(t))|$.

(5) Adjust the strong motion records. The strong motion records are adjusted in the frequency domain based on the frequency domain amplification coefficient curve. First, motion records are subjected to a Fourier Transform (FT). Then, the amplitudes of different frequency bands are adjusted according to the frequency adjustment coefficient curve:

$$\tilde{A}_{adj}(f) = \frac{\tilde{A}_{rec}(f)}{\zeta(f)}, \quad (11)$$

where $\tilde{A}_{rec}(f)$ represents the frequency-domain amplitude of the original seismic record, and $\zeta(f)$ is the frequency adjustment coefficient mentioned above.

Finally, the adjusted frequency-domain amplitude is restored to the time-domain signal through the inverse Fourier transform (IFT), resulting in the adjusted incident wave field.

To better explain this method, a single-layer soil body is analyzed in this section, with parameters $h = 20$ m, $v_s = 500$ m/s, $\rho = 1914$ kg/m³, $\xi = 0.0866$. The whole adjustment process is shown in Fig. 3. Firstly, the response of the soil bottom under different frequency sine wave input is calculated, and the gray curve represents the bottom response in the response results. The blue and orange curves represent the sine wave input from the bottom and the reflected wave transmitted to the bottom, respectively. After the response reaches the steady state, obtain the adjustment coefficient ξ corresponding to different sine wave frequencies, such as $f_i = 1$ Hz, $\zeta(2.5 \text{ Hz}) = 1.705$. By dividing the amplitude of each frequency band of the recorded seismic wave by the adjustment coefficient of the corresponding frequency band, the approximate incident wave can be obtained. In the lower right corner of Fig. 3, the whole adjustment process is shown.

The process of obtaining the frequency coefficient curve for the multi-layer soil model is similar to that of the single-layer soil model. By inputting sine waves of different frequencies as the initial signal and recursively calculating the reflected and transmitted waves at each layer using wave theory, the response at the bottom of the soil is obtained. For instance, consider a two-layer soil system, as shown in Fig. 4(a). Using an incident sine wave with a frequency of $f_i = 6$ Hz as an example, the calculation and adjustment process is depicted in Fig. 4(c) and Fig. 4(d). After adjusting the sine wave in the frequency range 0 to 25 Hz, the frequency adjustment coefficient ζ for the range 0 to 25 Hz can be obtained, as shown in Fig. 4(b). For a clearer explanation, we have presented a flowchart of the entire adjustment process, as shown in Fig. 5.

For different reflection truncation tolerances and different damping, the amplification factor curve will be different. Fig. 5 shows the influence of different reflection truncation tolerances and different multiples relative to the original damping on the adjustment coefficient by taking the

multi-layer soil model in the above article as an example.

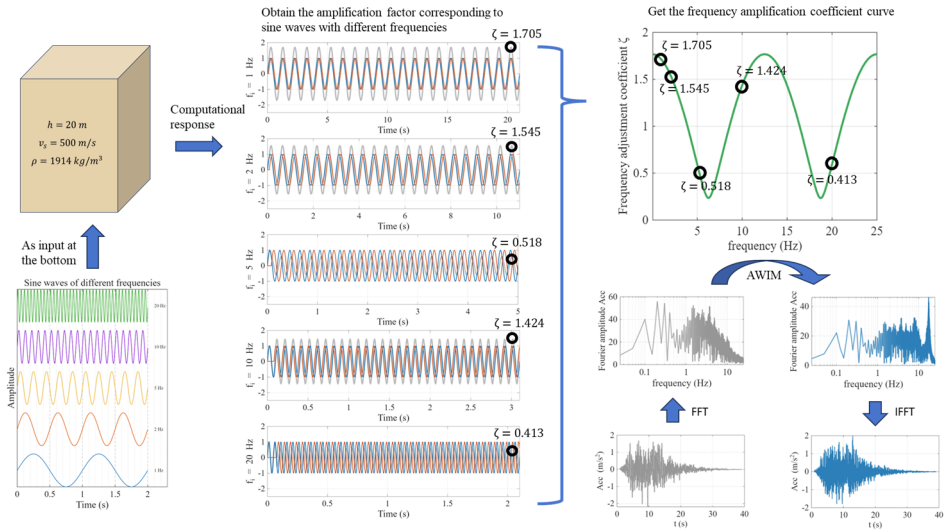


Fig. 3. AWIM step

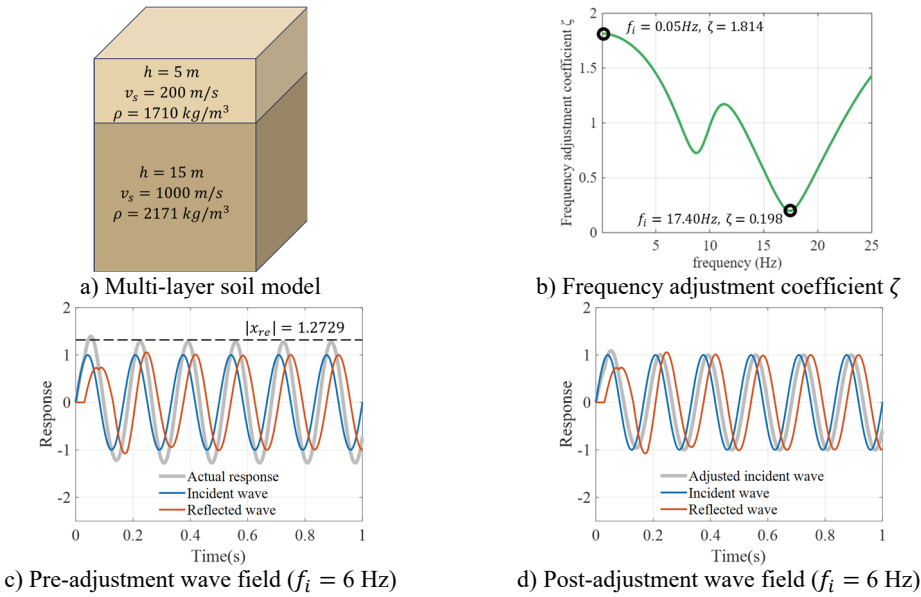


Fig. 4. Multi-layer soil frequency adjustment coefficient and adjustment process

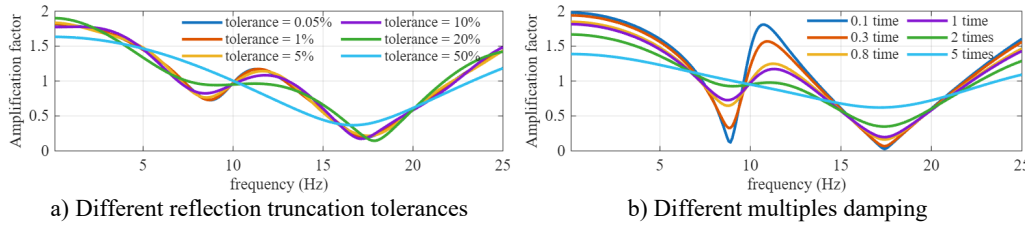


Fig. 5. The influence of different reflection truncation tolerances and different multiples relative to the original damping on the adjustment coefficient

3. Conclusions

A frequency-domain adjusted wave input method (AWIM) to bridge the gap between recorded strong-motion records (total wave field) and the incident wave field required for one-dimensional site response analysis was proposed. By employing wave propagation theory and recursive layer calculations, site-specific frequency adjustment coefficients ζ are derived to effectively link the incident wave field with the recorded strong-motion data. The advantage of this method is that the incident wave can be obtained without including the reflected part. The results show that both single-layer and multi-layer sites exhibit significant amplification effects on low-frequency incident waves, with amplification factors close to 2. For other frequency bands, the soil shows complex amplification and attenuation effects. In single-layer soil, these effects display a clear periodic pattern related to the shear wave velocity of the soil. However, in multi-layer soil, such periodicity is less evident.

Acknowledgements

The authors have not disclosed any funding.

Data availability

The datasets generated during and/or analyzed during the current study are available from the corresponding author on reasonable request.

Conflict of interest

The authors declare that they have no conflict of interest.

References

- [1] Y.-B. Wang, X.-S. Huang, and C. Li, "The truncation effect of soil slope acceleration responses," *Soil Dynamics and Earthquake Engineering*, Vol. 190, p. 109099, Mar. 2025, <https://doi.org/10.1016/j.soildyn.2024.109099>
- [2] K. Mahmood, Z.-U.- Rehman, K. Farooq, and S. A. Memon, "One dimensional equivalent linear ground response analysis – A case study of collapsed Margalla Tower in Islamabad during 2005 Muzaffarabad Earthquake," *Journal of Applied Geophysics*, Vol. 130, pp. 110–117, Jul. 2016, <https://doi.org/10.1016/j.jappgeo.2016.04.015>
- [3] M. Koolivand, R. R. Ardakani, A. Mahdavian, and H. Saffari, "Simulation of the 2016 Kumamoto earthquakes using the finite element method with concentrated friction," *KSCE Journal of Civil Engineering*, Vol. 27, No. 9, pp. 3824–3835, Sep. 2023, <https://doi.org/10.1007/s12205-023-0031-2>
- [4] K. Koketsu, B. L. N. Kennett, and H. Takenaka, "2-D reflectivity method and synthetic seismograms for irregularly layered structures-II. Invariant embedding approach," *Geophysical Journal International*, Vol. 105, No. 1, pp. 119–130, Apr. 1991, <https://doi.org/10.1111/j.1365-246x.1991.tb03448.x>
- [5] Z. Shan, L. Jing, L. Zhang, Z. Xie, and D. Ling, "Transient wave propagation in a multi-layered soil with a fluid surface layer: 1D analytical/semi-analytical solutions," *International Journal for Numerical and Analytical Methods in Geomechanics*, Vol. 45, No. 13, pp. 2001–2015, Jun. 2021, <https://doi.org/10.1002/nag.3253>